Electronic Supplementary Material (ESI) for Physical Chemistry Chemical Physics.
This journal is © the Owner Societies 2016

Supporting Information for

Molecular Conformation of DPPC Phospholipid Langmuir and Langmuir-Blodgett Monolayers Studied by Heterodyne-Detected Vibrational Sum Frequency Generation Spectroscopy

Naoki Takeshita, Masanari Okuno, and Taka-aki Ishibashi*[a]

[a] *Department of Chemistry, Graduate School of Pure and Applied Sciences, University of Tsukuba, 1-1-1 Tennodai, Tsukuba, Ibaraki 305-8571 Japan*

Spectral Analysis.

Fig. S1a shows the raw intensity spectra from a DPPC Langmuir monolayer on water at 45 mN/m and a reference left-handed *z*-cut quartz plate, respectively. The total signal I is expressed as,

$$I \propto |\tilde{E}_{\text{total}}|^2 = |\tilde{E}_{\text{sample}}|^2 + |\tilde{E}_{\text{LO}}|^2 + \tilde{E}^*_{\text{sample}}\tilde{E}_{\text{LO}}\exp(\mathrm{i}\omega T) + \tilde{E}_{\text{sample}}\tilde{E}^*_{\text{LO}}\exp(-\mathrm{i}\omega T) \qquad (1)$$

The interference terms, the third and fourth terms in eqn (1), give rise to the interference fringe pattern seen in Fig. S1a. The spectra are inverse-Fourier transformed into the time domain (real parts are shown in Fig. S1b). By applying a filter function shown in Fig. S1b, the interference term at $t = -T = -2.5$ ps, which corresponds to the fourth term in eqn (1), is extracted from the time-domain

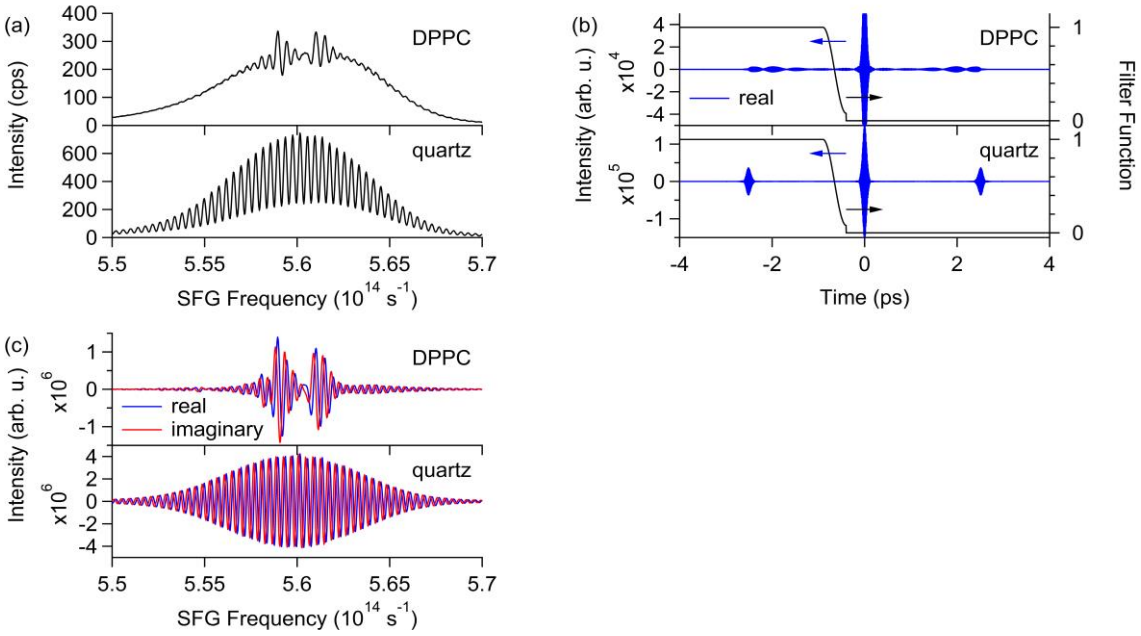

Fig. S1 (a) Raw intensity spectra from the air/DPPC monolayer on water (45 mN/m) interface and air/quartz interface. (b) Real parts (blue) of the time-domain interferogram and the filter function used in this study (black). The left axis is for the interferogram and the right axis is for the filter function. (c) Real and imaginary parts of the filtered spectra.

interferogram. A combination of a boxcar function and a Happ-Genzel function,

$$A(t) = 0.54 + 0.46\cos\left[\frac{\pi(t + 0.9\ \text{ps})}{0.5\ \text{ps}}\right] \quad (2)$$

was used as the filter function. The Fourier transformation of the filtered interferogram gives the complex spectra of the fourth term in eqn (1) (shown in Fig. S1c).

Fresnel Coefficients.

The diagonal elements of the Fresnel factors (L_{II}) are given by,[1]

$$L_{XX} = \frac{2n_1\cos\theta_2}{n_1\cos\theta_2 + n_2\cos\theta_1}$$
$$L_{YY} = \frac{2n_1\cos\theta_1}{n_1\cos\theta_1 + n_2\cos\theta_2} \quad (3)$$
$$L_{ZZ} = \frac{2n_2\cos\theta_1}{n_1\cos\theta_2 + n_2\cos\theta_1}\left(\frac{n_1}{n'}\right)^2$$

where n_1 and n_2 are the refractive indices of air and the support substrate of the monolayer, θ_1 and θ_2 are the incident and refracted angles of the beams, and n' is the refractive index of the interfacial layer, respectively. In this study, we calculated the refractive index of the interfacial layer n' according to a literature.[1] The Fresnel factors were calculated by using the parameters listed in Table S1 and S2. The dispersion and imaginary parts of n_2 were neglected in the calculation because they have little effect on the Fresnel factors in the CH stretching region.

Table S1 Parameters used to calculate Fresnel factors for the air/water interface

	ω_{SFG}	ω_{VIS}	ω_{IR}
λ (nm)	532	630	3400
n_2 [2]	1.334	1.332	1.432
θ_1 (deg.)	71	73	62
L_{YY}	0.52	0.49	0.59
L_{ZZ}	0.58	0.55	0.65

Table S2 Parameters used to calculate Fresnel factors for the air/fused silica interface

	ω_{SFG}	ω_{VIS}	ω_{IR}
λ (nm)	532	630	3400
n_2 [3]	1.461	1.457	1.410
θ_1 (deg.)	71	73	62
L_{YY}	0.46	0.43	0.60
L_{ZZ}	0.54	0.51	0.66

Effective Nonlinear Susceptibility of Crystalline Quartz.

In our experiment, a left-handed *z*-cut quartz was used as our reference sample. The SFG signal from a crystalline quartz plate is mainly from the bulk, which has D_3 symmetry with the nonvanishing $\chi^{(2)}_{ijk}$ elements,

$$\begin{aligned}
&\chi^{(2)}_{xxx} = -\chi^{(2)}_{xyy} = -\chi^{(2)}_{yyx} = -\chi^{(2)}_{yxy} \equiv \chi^{(2)}_{\mathrm{q}} \\
&\chi^{(2)}_{xyz} = -\chi^{(2)}_{yxz} \\
&\chi^{(2)}_{xzy} = -\chi^{(2)}_{yzx} \\
&\chi^{(2)}_{zxy} = -\chi^{(2)}_{zyx}
\end{aligned} \tag{4}$$

Among these factors, $\chi^{(2)}_{xxx}$ (defined as $\chi^{(2)}_{\mathrm{q}}$) and those equal to $\chi^{(2)}_{xxx}$ are much larger than the others.[4] In the following calculation, we neglected the weaker ones. In our experimental configuration, where the *x* and *z* axes of the quartz coincide with the *X* and *Z* axes of the laboratory coordinate, the effective second-order nonlinear susceptibilities observed in the SSP, PPP, and SPS polarization combinations can be expressed as,[4,5]

$$\begin{aligned}
\chi^{(2)}_{\mathrm{eff,SSP}} &= \cos\theta_{\mathrm{IR}} L_{YY}(\omega_{\mathrm{SFG}}) L_{YY}(\omega_{\mathrm{VIS}}) L_{XX}(\omega_{\mathrm{IR}}) \chi^{(2)}_{\mathrm{q}} l_c \\
\chi^{(2)}_{\mathrm{eff,PPP}} &= \cos\theta_{\mathrm{SFG}} \cos\theta_{\mathrm{VIS}} \cos\theta_{\mathrm{IR}} L_{XX}(\omega_{\mathrm{SFG}}) L_{XX}(\omega_{\mathrm{VIS}}) L_{XX}(\omega_{\mathrm{IR}}) \chi^{(2)}_{\mathrm{q}} l_c \\
\chi^{(2)}_{\mathrm{eff,SPS}} &= \cos\theta_{\mathrm{VIS}} L_{YY}(\omega_{\mathrm{SFG}}) L_{XX}(\omega_{\mathrm{VIS}}) L_{YY}(\omega_{\mathrm{IR}}) \chi^{(2)}_{\mathrm{q}} l_c
\end{aligned} \tag{5}$$

where θ and L_{II} are the incidence angles and Fresnel factors, both listed in Table S3, and l_c is the effective coherence length for the reflected SFG. In the present experiment,

$$l_c = \frac{1}{k_{2Z}(\omega_{\mathrm{SFG}}) + k_{2Z}(\omega_{\mathrm{VIS}}) + k_{2Z}(\omega_{\mathrm{IR}})} \approx 35\ \mathrm{nm} \tag{6}$$

where *k*'s are the wave vectors of the beams. Since the SFG signal from crystalline quartz is far from resonances in our experiment, we may neglect the dispersion and take

$$\chi^{(2)}_{\mathrm{q}} = 2d_{11} \approx 6.0\times10^{-13}\ \mathrm{m\ V^{-1}} \tag{7}$$

Here, d_{11} refers to the nonlinear coefficient of quartz for SHG, and its value for λ = 0.532 μm found in the literature[6] was used. We then calculated the effective second-nonlinear susceptibilities in our case, from the parameters listed in Table S3 and eqn (5),

$$\begin{aligned}
\chi^{(2)}_{\mathrm{eff,SSP}} &= 1.78\times10^{-21}\ \mathrm{m^2\ V^{-1}} \\
\chi^{(2)}_{\mathrm{eff,PPP}} &= 1.60\times10^{-21}\ \mathrm{m^2\ V^{-1}} \\
\chi^{(2)}_{\mathrm{eff,SPS}} &= 1.89\times10^{-21}\ \mathrm{m^2\ V^{-1}}
\end{aligned} \tag{8}$$

For convenience the birefringence of quartz was neglected, and the refractive index of the ordinary wave n_o was used for all polarizations.[4]

Table S3 Parameters used to calculate $\chi^{(2)}_{\mathrm{eff}}$ of a left-handed *z*-cut quartz

	ω_{SFG}	ω_{VIS}	ω_{IR}
λ (nm)	532	630	3400
$n_{o,2}$ [3]	1.547	1.543	1.49
θ_1 (deg.)	71	73	62
L_{XX}	1.20	1.27	1.07
L_{YY}	0.44	0.39	0.56

Reflectivities.

The reflectivities for S and P polarized beams are given by

$$r_{\mathrm{S}} = \frac{n_1 \cos\theta_1 - n_2 \cos\theta_2}{n_1 \cos\theta_1 + n_2 \cos\theta_2}$$
$$r_{\mathrm{P}} = \frac{-n_1 \cos\theta_2 + n_2 \cos\theta_1}{n_1 \cos\theta_2 + n_2 \cos\theta_1} \quad (9)$$

By using the parameters listed in Table S1, S2 and S3, the reflectivities of the LO at the air/water, air/fused silica, and air/quartz interfaces in our case were

$$r_{\mathrm{S,water}} = -0.48$$
$$r_{\mathrm{P,water}} = -0.23$$
$$r_{\mathrm{S,fused\ silica}} = -0.54$$
$$r_{\mathrm{P,fused\ silica}} = -0.22 \quad (10)$$
$$r_{\mathrm{S,quartz}} = -0.57$$
$$r_{\mathrm{P,quartz}} = -0.21$$

Fitted $\mathrm{Re}[\chi^{(2)}_{\mathrm{eff,SSP}}]$ spectra and the fitting parameters.

In the spectral fitting, we simultaneously fitted the imaginary and real parts of $\chi^{(2)}_{\mathrm{eff}}$ to eqn (3) in the main text. Fig. S2a and S2b show the fitted $\mathrm{Re}[\chi^{(2)}_{\mathrm{eff}}]$ spectra in the SSP polarization combination of DPPC monolayer on water and on the fused silica substrates, respectively.

The fitting parameters are listed in Table S4 and S5. "–" in the tables denotes that the band was not assumed in the fitting of the corresponding spectra. Since the fitted spectra are the difference spectra of DPPC and d_{62}-DPPC monolayers, it is likely that the nonresonant background was almost canceled out in them. Thus the non-zero amplitudes of the nonresonant background are probably due to an experimental error. In this study, since they are 2 orders smaller than the amplitudes of the resonant signals, the error does not affect the orientation analysis.

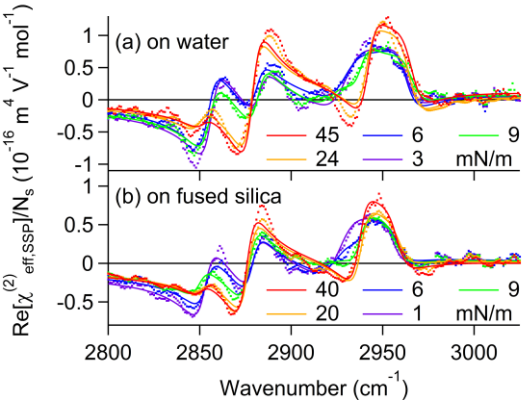

Fig. S2 Fitting results of Re[$\chi^{(2)}$] spectra of DPPC Langmuir monolayer on water (a) and LB monolayer on fused silica (b). In all observed spectra (dots), the corresponding Re[$\chi^{(2)}$] spectra of d_{62}-DPPC monolayer are already subtracted. Solid lines are spectral fits.

Table S4 Fitting parameters of $\chi^{(2)}_{\mathrm{eff,SSP}}$ spectra of Langmuir monolayers on water

		surface pressure (mN/m)				
		3	6	9	24	45
$\chi^{(2)}_{\mathrm{NR}}$ ($\mathrm{m^4\ V^{-1}\ mol^{-1}}$)		-3.85×10^{-18}	-7.87×10^{-21}	-3.15×10^{-18}	7.35×10^{-20}	3.94×10^{-18}
CH_2 ss	ω ($\mathrm{cm^{-1}}$)	2856	2855	2855	2850	2852
	Γ ($\mathrm{cm^{-1}}$)	7	7	7	7	7
	$A_{\mathrm{eff,SSP}}$ [a]	2.50×10^{-5}	2.23×10^{-5}	1.88×10^{-5}	6.51×10^{-6}	4.02×10^{-6}
CH_3 ss	ω ($\mathrm{cm^{-1}}$)	2883	2881	2882	2879	2879
	Γ ($\mathrm{cm^{-1}}$)	6	6	6	6	6
	$A_{\mathrm{eff,SSP}}$	1.14×10^{-5}	1.29×10^{-5}	1.56×10^{-5}	3.02×10^{-5}	3.35×10^{-5}
CH_2 FR	ω ($\mathrm{cm^{-1}}$)	2930	2930	2923	–	–
	Γ ($\mathrm{cm^{-1}}$)	13	13	13	–	–
	$A_{\mathrm{eff,SSP}}$	1.34×10^{-5}	1.14×10^{-5}	1.54×10^{-5}	–	–
CH_3 FR	ω ($\mathrm{cm^{-1}}$)	–	–	2938	2941	2942
	Γ ($\mathrm{cm^{-1}}$)	–	–	7	7	7
	$A_{\mathrm{eff,SSP}}$	–	–	1.52×10^{-5}	1.00×10^{-5}	1.15×10^{-5}
CH_3 as	ω ($\mathrm{cm^{-1}}$)	2963	2963	2966	2964	2966
	Γ ($\mathrm{cm^{-1}}$)	9	9	9	9	9
	$A_{\mathrm{eff,SSP}}$	-1.59×10^{-5}	-1.77×10^{-5}	-1.35×10^{-5}	-2.39×10^{-5}	-2.19×10^{-5}

[a] The unit of A is $\mathrm{m^4\ V^{-1}\ s^{-1}\ mol^{-1}}$.

Table S5 Fitting parameters of $\chi^{(2)}_{\mathrm{eff,SSP}}$ spectra of LB monolayers on fused silica

		surface pressure (mN/m)				
		1	6	9	20	40
$\chi^{(2)}_{\mathrm{NR}}$ ($\mathrm{m^4\ V^{-1}\ mol^{-1}}$)		-6.96×10^{-18}	-5.00×10^{-18}	-3.60×10^{-18}	-5.20×10^{-18}	-5.25×10^{-18}
CH_2 ss	ω ($\mathrm{cm^{-1}}$)	2853	2853	2850	2851	2851
	Γ ($\mathrm{cm^{-1}}$)	7	7	7	7	7
	$A_{\mathrm{eff,SSP}}$ [a]	1.66×10^{-5}	1.15×10^{-5}	6.61×10^{-6}	3.52×10^{-6}	3.40×10^{-6}
CH_3 ss	ω ($\mathrm{cm^{-1}}$)	2879	2879	2877	2877	2876
	Γ ($\mathrm{cm^{-1}}$)	6	6	6	6	6
	$A_{\mathrm{eff,SSP}}$	1.18×10^{-5}	1.26×10^{-5}	1.58×10^{-5}	2.02×10^{-5}	2.26×10^{-5}
CH_2 FR	ω ($\mathrm{cm^{-1}}$)	2927	2925	2923	–	–
	Γ ($\mathrm{cm^{-1}}$)	13	13	13	–	–
	$A_{\mathrm{eff,SSP}}$	2.59×10^{-5}	1.68×10^{-5}	7.81×10^{-6}	–	–
CH_3 FR	ω ($\mathrm{cm^{-1}}$)	–	2939	2938	2938	2937
	Γ ($\mathrm{cm^{-1}}$)	–	7	7	7	7
	$A_{\mathrm{eff,SSP}}$	–	5.49×10^{-6}	1.01×10^{-5}	1.64×10^{-5}	1.83×10^{-5}
CH_3 as	ω ($\mathrm{cm^{-1}}$)	2956	2958	2957	2959	2958
	Γ ($\mathrm{cm^{-1}}$)	9	9	9	9	9
	$A_{\mathrm{eff,SSP}}$	-1.11×10^{-5}	-9.03×10^{-6}	-9.87×10^{-6}	-9.93×10^{-6}	-1.50×10^{-5}

[a] The unit of A is $\mathrm{m^4\ V^{-1}\ s^{-1}\ mol^{-1}}$.

Orientation Analysis Using $\chi^{(2)}_{\mathrm{eff,SPS}}$ Spectra.

In the previous homodyne-detected VSFG studies,[7,8] the ratio of the amplitudes for the CH_3 as band at ~2960 $\mathrm{cm^{-1}}$ in the SSP and SPS polarization combinations was commonly used to calculate the tilt angle of terminal methyl groups of alkyl chains. However, we think that this method cannot offer reliable parameters for the orientation calculation in our case. This is because the $\chi^{(2)}$ spectra in the SPS polarization are too congested to extract accurate parameters of each band. In particular, a positive spectral feature around 2935 $\mathrm{cm^{-1}}$, which we first observed, is difficult to reproduce as shown in later.

Therefore, we determined approximate parameters for CH_3 as band in the SPS spectra in the following way, as support for the methyl group orientation discussed in the main text. To remove the contribution of the head group and the subphase water to the spectra, $\chi^{(2)}$ spectra of d_{62}-DPPC monolayer were subtracted from the $\chi^{(2)}$ spectra of DPPC monolayer on the corresponding substrates and in corresponding phases. We fitted the subtracted spectra in the frequency region of 2950–2975 $\mathrm{cm^{-1}}$, using eqn (3) in the main text, assuming one vibrational mode. ω_q's and Γ_q's for all the spectra are fixed to be the value determined in the SSP polarization combination. Spectral fits are shown in

Fig. S3a and S3b. Even though the fits cannot reproduce the spectral region around 2935 cm^{-1}, we can still discuss the molecular orientations in a qualitative way. The fitting parameters are listed in Table S6 and S7. As mentioned in the fitting analysis of $\chi^{(2)}_{\mathrm{eff,SSP}}$ spectra, although the non-zero amplitudes of the nonresonant background are probably ascribed to an experimental error, they are 2 orders smaller than the peak heights of the resonant signals, and thus they do not affect the orientation analysis.

The effective second-order nonlinear susceptibility measured in the SPS polarization combination ($\chi^{(2)}_{\mathrm{eff,SPS}}$) is connected to the $\chi^{(2)}_{YZY}$ element of the second-order nonlinear susceptibility in the lab coordinate,[1]

$$\chi^{(2)}_{\mathrm{eff,SPS}} = L_{YY}(\omega_{\mathrm{SFG}})L_{ZZ}(\omega_{\mathrm{VIS}})L_{YY}(\omega_{\mathrm{IR}})\sin\theta_{1,\mathrm{VIS}}\chi^{(2)}_{YZY} \quad (11)$$

where $\theta_{1,\mathrm{VIS}}$ is the incidence angle of the visible beam, and L_{YY} and L_{ZZ} are the diagonal elements of the Fresnel factors.

When we assume C_{3v} symmetry of the terminal methyl group, a δ function distribution of methyl group tiling angle (θ), and an azimuthally isotropic surface, $\chi^{(2)}_{YYZ}$ and $\chi^{(2)}_{YZY}$ elements of CH_3 as mode are expressed as,[7]

$$\chi^{(2)}_{YYZ}(\mathrm{CH_3\ as}) = -\frac{1}{2}N_s\beta_{caa}(\cos\theta - \cos^3\theta) \quad (12)$$

$$\chi^{(2)}_{YZY}(\mathrm{CH_3\ as}) = \frac{1}{2}N_s\beta_{caa}\cos^3\theta \quad (13)$$

Here, N_s is the surface molecular density and β_{caa} is the tensor element of the molecular hyperpolarizability. From eqn (12) and (13), it can be shown that

$$\frac{\chi^{(2)}_{YYY}(\mathrm{CH_3\ as})}{\chi^{(2)}_{YZY}(\mathrm{CH_3\ as})} = -\frac{\cos\theta - \cos^3\theta}{\cos^3\theta} \quad (14)$$

The $\chi^{(2)}_{YYZ}(\mathrm{CH_3\ ss}) / \chi^{(2)}_{YZY}(\mathrm{CH_3\ as})$ ratio is shown in Fig. S4 as a function of θ.

Fig. S3e depicts the amplitude ratio of CH_3 as band in SSP and SPS polarization combination against the surface pressure. For both monolayers on water and on the fused silica substrates, the ratios increased when the surface pressure increased. Moreover, the ratio for the monolayer on fused silica was larger than that for the monolayer on water in the whole region. According to Fig. S4, the increase of the ratio can be interpreted as a decrease in the tilt angle.

In the main text, the difference of the amplitude ratio of CH_3 ss and CH_3 as between the monolayer on water and on fused silica was small above ~40 mN/m. Contrastingly, the difference of the amplitude ratio of CH_3 as band in SSP and SPS polarization combinations was significant. This might be due to the fitting errors or the experimental errors in the SPS spectra. Nevertheless, our result in the SPS polarization combination supposedly indicates that the methyl groups of the Langmuir-Blodgett monolayers deposited on the fused silica substrates tend to be less tilted from the surface normal than the Langmuir monolayers on water.

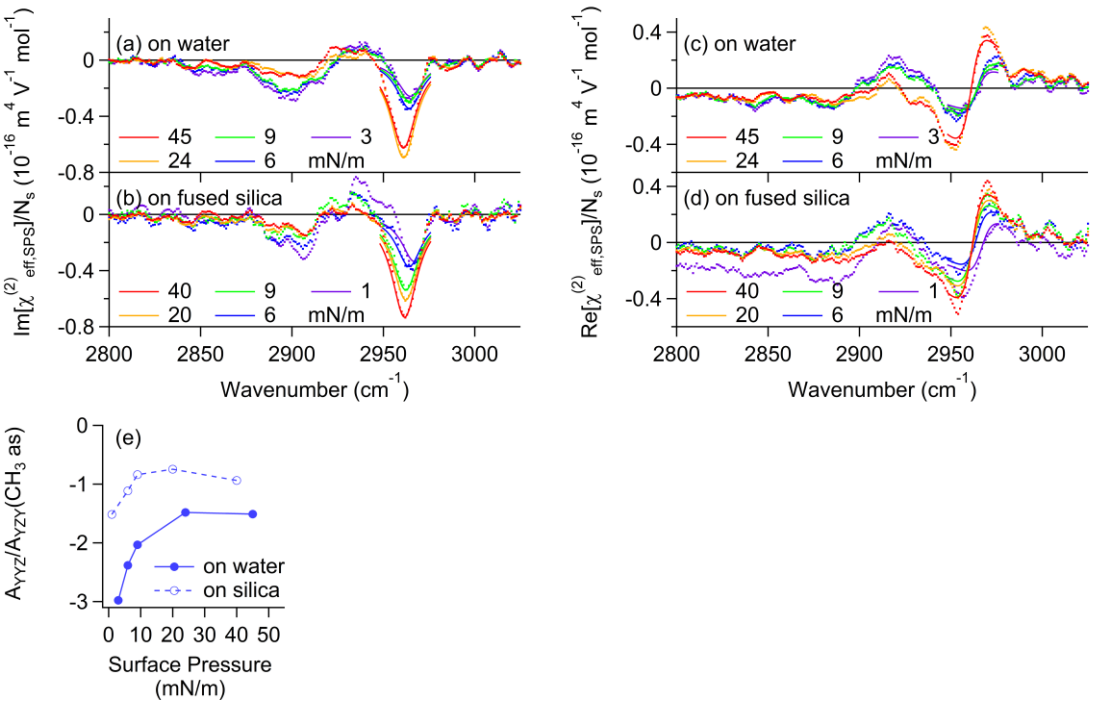

Fig. S3 Fitting results of $\chi^{(2)}$ spectra in the SPS polarization combination of DPPC Langmuir monolayer on water (a, c) and LB monolayer on fused silica (b, d). In all observed spectra (dots), the corresponding $\chi^{(2)}$ spectra of d_{62}-DPPC monolayer are already subtracted. Solid lines are spectral fits. (c) The ratio of amplitudes for CH_3 as band in the SSP and SPS polarization combinations as a function of surface pressure.

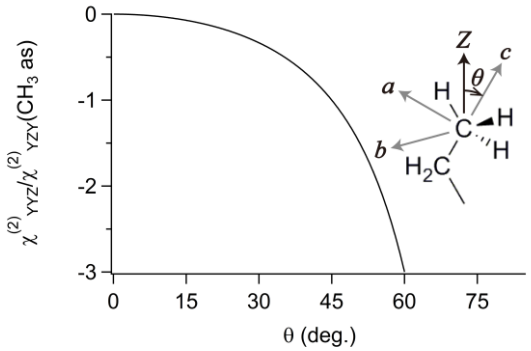

Fig. S4 Relationship between calculated $\chi^{(2)}_{YYZ}(CH_3\ ss) / \chi^{(2)}_{YYZ}(CH_3\ as)$ ratio of CH_3 ss and CH_3 as bands and the tilt angle of the methyl group. Inset shows the definition of θ.

Table S6 Fitting parameters of $\chi^{(2)}_{\mathrm{eff,SPS}}$ spectra of Langmuir monolayers on water

		surface pressure (mN/m)				
		3	6	9	24	45
$\chi^{(2)}_{\mathrm{NR}}$ ($\mathrm{m^4\ V^{-1}\ mol^{-1}}$)		-1.34×10^{-18}	-6.97×10^{-19}	-9.04×10^{-19}	-8.10×10^{-19}	-2.15×10^{-18}
CH_3 as	ω ($\mathrm{cm^{-1}}$)	2963	2963	2966	2964	2966
	Γ ($\mathrm{cm^{-1}}$)	9	9	9	9	9
	$A_{\mathrm{eff,SPS}}$ [a]	6.60×10^{-6}	8.81×10^{-6}	7.49×10^{-6}	1.78×10^{-5}	1.61×10^{-5}

[a] The unit of A is $\mathrm{m^4\ V^{-1}\ s^{-1}\ mol^{-1}}$.

Table S7 Fitting parameters of $\chi^{(2)}_{\mathrm{eff,SPS}}$ spectra of LB monolayers on fused silica

		surface pressure (mN/m)				
		1	6	9	20	40
$\chi^{(2)}_{\mathrm{NR}}$ ($\mathrm{m^4\ V^{-1}\ mol^{-1}}$)		-3.36×10^{-18}	-3.07×10^{-18}	-6.04×10^{-19}	-4.11×10^{-19}	-2.62×10^{-18}
CH_3 as	ω ($\mathrm{cm^{-1}}$)	2956	2958	2957	2959	2958
	Γ ($\mathrm{cm^{-1}}$)	9	9	9	9	9
	$A_{\mathrm{eff,SPS}}$ [a]	8.58×10^{-6}	9.52×10^{-6}	1.38×10^{-5}	1.56×10^{-5}	1.88×10^{-5}

[a] The unit of A is $\mathrm{m^4\ V^{-1}\ s^{-1}\ mol^{-1}}$.

References

1 X. Zhuang, P. Miranda, D. Kim and Y. R. Shen, Phys. Rev. B, 1999, **59**, 12632–12640.

2 G. M. Hale and M. R. Querry, Appl. Opt., 1973, **12**, 555–563.

3 E. D. Palik, Handbook of Optical Constants of Solids, Academic Press, San Diego, 1985.

4 X. Wei, S. Hong, X. Zhuang, T. Goto and Y. R. Shen, Phys. Rev. E, 2000, **62**, 5160–5172.

5 Y. R. Shen, The Principles of Nonlinear Optics, Wiley, New York, 1984.

6 I. Shoji, T. Kondo, A. Kitamoto, M. Shirane and R. Ito, J. Opt. Soc. Am. B, 1997, **14**, 2268–2294.

7 J. Wang, C. Chen, S. M. Buck and Z. Chen, J. Phys. Chem. B, 2001, **105**, 12118–12125.

8 J. Kim and G. A. Somorjai, J. Am. Chem. Soc., 2003, **125**, 3150–3158.